

# SPINT2 is involved in the proliferation, migration and phenotypic switching of aortic smooth muscle cells: Implications for the pathogenesis of thoracic aortic dissection

JUN LI<sup>1</sup>, CHANGJUN YU<sup>2</sup>, KANGMIN YU<sup>1</sup>, ZHIYONG CHEN<sup>1</sup>,  
DAN XING<sup>3</sup>, BINSHAN ZHA<sup>1</sup>, WENTAO XIE<sup>1</sup> and HUAN OUYANG<sup>1</sup>

Departments of <sup>1</sup>Vascular Surgery, <sup>2</sup>Gastrointestinal Surgery and <sup>3</sup>Medical Record Management,  
The First Affiliated Hospital of Anhui Medical University, Hefei, Anhui 230022, P.R. China

Received January 17, 2023; Accepted August 25, 2023

DOI: 10.3892/etm.2023.12245

**Abstract.** Thoracic aortic dissection (TAD) is a severe and extremely dangerous cardiovascular disease. Proliferation, migration and phenotypic switching of vascular smooth muscle cells (SMCs) are major pathogenetic mechanisms involved in the development of TAD. The present study was designed to investigate the expression and potential function of serine peptidase inhibitor Kunitz type 2 (SPINT2) in TAD. The gene expression profile data for ascending aorta from patients with TAD were downloaded from the GEO database with the accession number GSE52093. Bioinformatics analysis using GEO2R indicated that the differentially expressed SPINT2 was prominently decreased in TAD. The expression levels of SPINT2 mRNA and protein in aortic dissection specimens and normal aorta tissues were measured using reverse transcription-quantitative PCR and western blotting. SPINT2 expression was downregulated in clinical samples from aortic dissection specimens of patients with TAD compared with the corresponding expression noted in tissues derived from patients without TAD. *In vitro*, platelet-derived growth factor BB (PDGF-BB) was applied to induce the isolated primary mouse aortic SMC phenotypic modulation (a significant upregulation in the expression levels of synthetic markers), and the SMCs were infected with the adenoviral vector, Ad-SPINT2, to construct SPINT2-overexpressed cell lines. SMC viability was detected by an MTT assay and SMC proliferation was detected via the presence of Ki-67-positive cells (immunofluorescence staining). To explore the effects of SPINT2 on SMC migration, a wound healing assay was conducted. ELISA and western

blotting assays were used to measure the content and expression levels of MMP-2 and MMP-9. The expression levels of vimentin, collagen I,  $\alpha$ -SMA and SM22 $\alpha$  were measured using western blotting. The PDGF-BB-induced proliferation and migration of SMCs were recovered by SPINT2 overexpression. The increase in the expression levels of SPINT2 reduced the expression levels of active matrix metalloproteinases (MMPs), MMP-2 and MMP-9. Overexpression of SPINT2 suppressed SMC switching from a contractile to a synthetic type, as evidenced by decreased vimentin and collagen I expression levels along with increased  $\alpha$ -smooth muscle actin and smooth muscle protein 22- $\alpha$  expression levels. Furthermore, activation of ERK was inhibited in SPINT2-overexpressing SMCs. A specific ERK agonist, 12-O-tetradecanoylphorbol-13-acetate, reversed the SPINT2-mediated inhibition of SMC migration and the phenotypic switching. Collectively, the data indicated that SPINT2 was implicated in the proliferation, migration and phenotypic switching of aortic SMCs, suggesting that it may be involved in TAD progression.

## Introduction

Thoracic aortic dissection (TAD) is a complex disease that occurs in cardiovascular surgery (1); it is one of the most perilous and catastrophic aortic syndromes due to its high morbidity rate, acute onset and rapid progression (2). TAD is characterized by the tearing of the layers of the arterial wall, causing blood to flow within the arterial wall and pass into a 'false lumen', forming two lumens inside and outside the vessel, and producing a dissection in the thoracic aorta (3). The outcomes of surgical repair following TAD are gradually improving. However, the mortality rates remains high and thus, early and accurate diagnosis is critical to determine the appropriate therapy (4).

Vascular smooth muscle cells (SMCs) are the major cell type within the aortic wall; dysregulation of SMC function contributes to the development of TAD (5). Under certain stimuli (such as single gene mutations and abnormal gene expression) (6), SMCs can transcend from a quiescent and differentiated state to a proliferative, migratory and remodeling state, which is often characterized by their phenotype

---

*Correspondence to:* Dr Changjun Yu, Department of Gastrointestinal Surgery, The First Affiliated Hospital of Anhui Medical University, 218 Jixi Road, Hefei, Anhui 230022, P.R. China  
E-mail: ycejfy@sina.com

**Key words:** serine peptidase inhibitor Kunitz type 2, thoracic aortic dissection, smooth muscle cells, proliferation, migration, phenotypic switching

switching from the contractile toward the synthetic state; this is considered to be a primary driver in the pathogenesis of TAD (7). In addition, extracellular matrix (ECM) protein degradation can weaken the aortic wall and destroy the structural integrity of the aorta, which leaves it vulnerable to dissection (8). Matrix metalloproteinases (MMPs) can degrade ECM proteins, playing an important role in ECM metabolism and aortic tissue remodeling, which may also be related to TAD progression (9).

Serine peptidase inhibitor Kunitz type 2 (SPINT2), also known as hepatocyte growth factor activator inhibitor type-2 (10), belongs to the Kunitz family of serine protease inhibitors. This protein is a potent inhibitor of hepatocyte growth factor (HGF) activator (HGFA) (11). HGF, also named scatter factor (SF), may improve cell viability and invasiveness, stimulate angiogenesis and function as a tumor progression factor (12). Met tyrosine kinase receptor is the HGF receptor; the HGF/Met pathway plays a prominent role in cell migration, survival, growth and cardiovascular remodeling following tissue injury (13). Notably, SPINT2 binds to and inactivates HGFA, impairing the conversion of inactive pro-HGF/SF into bioactive HGF/SF (14). SPINT2 may therefore play an important role in cancer cell biology by regulating the function of HGF/SF-activating proteases. Previously, it was reported that SPINT2 overexpression could suppress pro-HGF activation, ECM degradation and prostate cancer cell invasion via its inhibitory effect on the proteolytic activity of these enzymes (15). SPINT2 regulates cell proliferation, migration and invasion via a reduction in HGFA, leading to apoptosis and necrosis of uterine leiomyosarcoma cells (16). Moreover, SPINT2 decreases cell migration and invasion abilities of glioma cells via downregulation of MMP-2 expression and activity (17) and reduces the levels of vimentin in endometrial cancer cells (18).

In the present study, dataset GSE52093, including 12 samples (7 TAD and 5 normal ascending tissues) was obtained from the Gene Expression Omnibus (GEO; <https://www.ncbi.nlm.nih.gov/geo/>) database and was analyzed by GEO2R (<https://www.ncbi.nlm.nih.gov/geo/geo2r/>). It was observed that SPINT2 expression was downregulated in the arterial tissues of patients with TAD. Therefore, the present study was designed to investigate the effects of SPINT2 on TAD progression by examining the role of SPINT2 in the proliferation, migration and phenotypic switching of aortic SMCs.

## Materials and methods

**Tissue specimen collection.** Aortic dissection specimens removed from patients with TAD (n=11) during surgery for TAD were collected. Control aortic specimens were obtained from patients undergoing coronary artery bypass grafting (n=4). All specimens were obtained from January 2022 to June 2022 at the First Affiliated Hospital of Anhui Medical University (Hefei, China). Patients who underwent computed tomography scans and ultrasonic examination to confirm the diagnosis of TAD were enrolled in the present study, whereas patients with connective tissue defects, such as bicuspid aortic valve malformation, traumatic aneurysms, luteic aortic aneurysms, or a family history of aortic diseases were excluded. The specimens were cleared of adventitia carefully

and subsequently used as fresh samples for western blotting and reverse transcription-quantitative PCR (RT-qPCR) analyses. And aortic dissection specimens were fixed with 4% paraformaldehyde for 15 min at room temperature for immunofluorescence (IF) staining. The present study was performed in accordance with the Declaration of Helsinki and approved by the Medical Ethics Committee of the First Affiliated Hospital of Anhui Medical University (approval no. Quick-PJ 2022-14-49). All participants signed an informed consent form prior to the present study.

**Primary aortic SMC isolation.** Male 6-week-old C57BL/6J mice weighing 18-22 g were purchased from the Experimental Animal Center of the First Affiliated Hospital of Anhui Medical University. A total of 8 mice were used in this experiment. The animals were housed in the Experimental Animal Center of the First Affiliated Hospital of Anhui Medical University under controlled conditions (temperature, 22±2°C; humidity, 40-60%) with a 12/12 h light/dark cycle and were provided with a normal diet with constant air renewal. The animal experimental procedures were performed with the approval of The Experimental Animal Ethics Committee of Anhui Medical University (approval no. LLSC20220940). The mice were sacrificed by intraperitoneal injection with sodium pentobarbital (150 mg/kg). Approximately 5×10<sup>6</sup> primary aortic SMCs were isolated from one mouse as described previously (19). Under sterile conditions, the excised aortic tissues were rinsed with PBS and excess tissues (such as fascia, all adherent fat and connective tissue) were removed using a surgical scalpel. The tissue pieces were digested with collagenase II (Biosharp Life Sciences) for 30 min at 37°C and the endothelia were gently removed. Subsequently, the cells were digested and collected using a mixture of collagenase II and elastase (Shanghai Aladdin Biochemical Technology Co., Ltd.) for 30 min at 37°C. The cells were allowed to reach a fusion state, cell passage was performed and the collected cells were maintained in smooth muscle cell medium (iCell Bioscience, Inc.) and cultured in an incubator at 37°C with 5% CO<sub>2</sub>. The SMCs used in this experiment were from the 3rd to 5th generations. SMCs were identified by IF staining of smooth muscle  $\alpha$ -actin ( $\alpha$ -SMA) and smooth muscle protein 22- $\alpha$  (SM22 $\alpha$ ).

**Bioinformatics analysis.** The gene expression profile data for ascending aorta from patients with TAD were downloaded from the GEO database with the accession number GSE52093. The dataset GSE52093 was based on the platform GPL10558, including 12 samples (7 TAD and 5 normal ascending tissues). GEO2R (<https://www.ncbi.nlm.nih.gov/geo/geo2r/>) and R software (R Development Core Team, version 4.1.2) were used to screen the differentially expressed genes (DEGs) between TAD and normal samples; P<0.05 and  $\log_2$  FC $\geq$ 1.5 were used as the screening thresholds. R packages ‘ggplot2’ and ‘pheatmap’ were utilized to yield the volcano plot and the heat map, respectively, for data visualization. The R software ‘cluster Profiler’ package was used to perform Gene Ontology (GO) functional enrichment, which was visualized with the chord plot. The Kyoto Encyclopedia of Genes and Genomes (KEGG) pathway (<https://www.genome.jp/kegg/>) was analyzed by gene set enrichment analysis (GSEA) used by R software ‘cluster Profiler’ package.

**Cell treatment and adenoviral infection.** The cells were treated with platelet-derived growth factor BB (PDGF-BB; GenScript) at different concentrations (0, 10, 20 and 40 ng/ml) for 24 h at 37°C to test SPINT2 expression and SMC viability. PDGF-BB at 20 ng/ml was selected to induce SMC phenotype modulation to establish the *in vitro* cell model. To explore the function of SPINT2, a 1st generation adenoviral system carrying the SPINT2 sequence was used to overexpress SPINT2 at a multiplicity of infection of 100 for 24 h in the isolated SMCs. The SPINT2 overexpressed sequence was synthesized by General Biological (Anhui) Co., Ltd. and ligated to the vector RedTrack-CMV (Fenghuishengwu, Co., Ltd.). The AdMax system was used. 293A cells (Saibaikang Biotechnology Co., Ltd.; iCell-h086) were used to package the adenovirus and cultured in DMEM containing 10% FBS at 37°C in a 5% CO<sub>2</sub> incubator. The 293A cells were cultured in a 10-cm culture dish, with a density of ~60% for transfection. First, 30 µl transfection reagent Lipofectamine 3000® (Thermo Fisher Scientific, Inc.) was diluted with 50 µl Opti-MEM (Thermo Fisher Scientific, Inc.). Next, 20 µg plasmids were diluted with 30 µl P3000 reagent in 500 µl Opti-MEM. The aforementioned two solutions were mixed and left at room temperature for 15 min. The mixed solution was transferred to the culture medium of the 293A cells, which were mixed and cultured in an incubator with 5% CO<sub>2</sub> at 37°C. When the plaque was ≥50% (~7 days), the cells and medium were collected into the centrifuge tube.

To verify the effect of SPINT2 on the activation of ERK, SMCs infected by adenovirus for 24 h were treated with 100 nmol/l 12-O-tetradecanoylphorbol-13-acetate (TPA; Beijing Solarbio Science & Technology Co., Ltd.) prior to treatment with 20 ng/ml PDGF-BB treatment.

**RT-qPCR.** Total RNA was extracted from tissue specimens and SMCs using the TRIpure reagent (BioTeke Corporation). Subsequently, cDNA was synthesized using M-murine leukemia virus reverse transcriptase (Beyotime Institute of Biotechnology) (incubate with 4 µl of RT buffer and 2 µl of dNTP for 50 min at 42°C, then terminate the reaction by heating at 80°C for 10 min). The PCR amplification was performed using SYBR Green reagent (Beijing Solarbio Science & Technology Co., Ltd.) on an Exicycler™ 96 Real-Time Quantitative PCR instrument (Bioneer Corporation). Thermocycling conditions were as follows: Initial denaturation for 5 min at 95°C, followed by 40 cycles of 10 sec at 95°C and 10 sec at 60°C, and extension at 72°C for 30 sec. The relative expression levels of SPINT2 mRNA were analyzed using the 2<sup>-ΔΔC<sub>q</sub></sup> method (20). The following primer sequences were used for analysis of the tissue specimens: *SPINT2* forward (F), 5'-AACGCAGCATCC ACGACT-3' and reverse (R), 5'-GGCACATTTCTTGAGGCA CT-3'. The following sequences were used for the analysis of SMCs: *SPINT2* F, 5'-GTGAAGGCAATGGCAATAAC-3' and R, 5'-ATAGTACCAGCGAGGGAAGG-3'.

**Western blotting analysis.** Aorta tissues or SMCs were lysed in RIPA lysis buffer (Beijing Solarbio Science & Technology Co., Ltd.) and sonicated for 5 min at 4°C at 14,000 rpm to extract the total proteins. The protein concentrations were quantified using the bicinchoninic protein assay kit (Beijing Solarbio Science & Technology Co., Ltd.). A total of 20 µg/lane protein

samples were separated by SDS-PAGE (Beijing Solarbio Science & Technology Co., Ltd.) on 10% gels and subsequently transferred onto polyvinylidene fluoride membranes (MilliporeSigma) by electroblotting. The membranes were blocked in 5% (M/V) non-fat milk powder for 1 h at room temperature and incubated with the primary antibodies overnight at 4°C. Subsequently, the horseradish peroxidase-labeled secondary antibody (1:3,000; cat. no. SE131/SE134; Beijing Solarbio Science & Technology Co., Ltd.) was incubated with the membranes at 37°C for 1 h. The bands on the membranes were visualized using an enhanced chemiluminescence reagent (Beijing Solarbio Science & Technology Co., Ltd.). The gray values of the target bands were analyzed using Tanon-5200 Image Analysis System (Tanon Science and Technology Co., Ltd.). The primary antibodies included anti-vimentin (1:1,000; cat. no. AF7013), anti-collagen I (1:1,000; cat. no. AF7001), anti-α-SMA (1:1,000; cat. no. AF1032), anti-SM22α (1:1,000; cat. no. AF9266), anti-MMP-9 (1:1,000; cat. no. AF5228), anti-p-ERK (1:500; cat. no. AF1015) and anti-ERK (1:500; cat. no. AF0155) antibodies (all Affinity Biosciences). Additionally, anti-MMP-2 (1:2,000; cat. no. 10373-2-AP; Proteintech Group, Inc.) and anti-SPINT2 (1:500; cat. no. sc-398119; Santa Cruz Biotechnology, Inc.) antibodies were used, and GAPDH (1:20,000; cat. no. 60004-1-Ig; ProteinTech Group, Inc.) was the internal control.

**3-(4,5-dimethylthiazol-2-yl)-2,5-diphenyltetrazolium bromide (MTT) assay.** SMCs were seeded into 96-well plates at a density of 4x10<sup>3</sup> cells/well. Following incubation overnight, SMCs were treated with different concentrations of PDGF-BB (0, 10, 20 and 40 ng/ml) for 24 h. Subsequently, 10 µl MTT reagent (Beyotime Institute of Biotechnology) was added into each well and incubated for an additional 4 h at 37°C. Dimethyl sulfoxide (100 µl) was added to each well to terminate the reaction, until it was observed under an ordinary optical microscope that the formazan was completely dissolved. Similarly, 20 ng/ml PDGF-BB or 20 ng/ml PDGF-BB + 100 nmol/l TPA was used to treat SMCs for 0, 24, 48 and 72 h, and MTT reagent was used to detect cell proliferation. Finally, the optical density values at 570 nm were measured with a microplate reader (BioTek Instruments, Inc.).

**Wound healing assay.** When the cells reached 90% confluence, the cell medium was altered to serum-free medium and 10 µg/ml mitomycin C (Merck KGaA). SMCs were scratched using 200-µl pipette tips. The cell surface was washed once with serum-free medium to remove cell debris. Subsequently, the cells of each group were incubated for 0 and 24 h in an incubator at 37°C with 5% CO<sub>2</sub> and the images were captured using an inverted microscope (Olympus Corporation) at a magnification of x100. Finally, the wound healing distance of SMCs was calculated to measure the cell migratory ability. Cell migration rate=(0 h scratch width-24 h scratch width)/0 h scratch width x100.

**ELISA.** The cell supernatants were centrifuged at 4°C for 10 min at 300 x g to remove the precipitate for detection. The mouse MMP-2 ELISA Kit (cat. no. EM0142; Wuhan Fine Biotech, Co., Ltd.) and the MMP-9 ELISA Kit [cat. no. EK2M09; Multisciences (Lianke) Biotech Co., Ltd.]

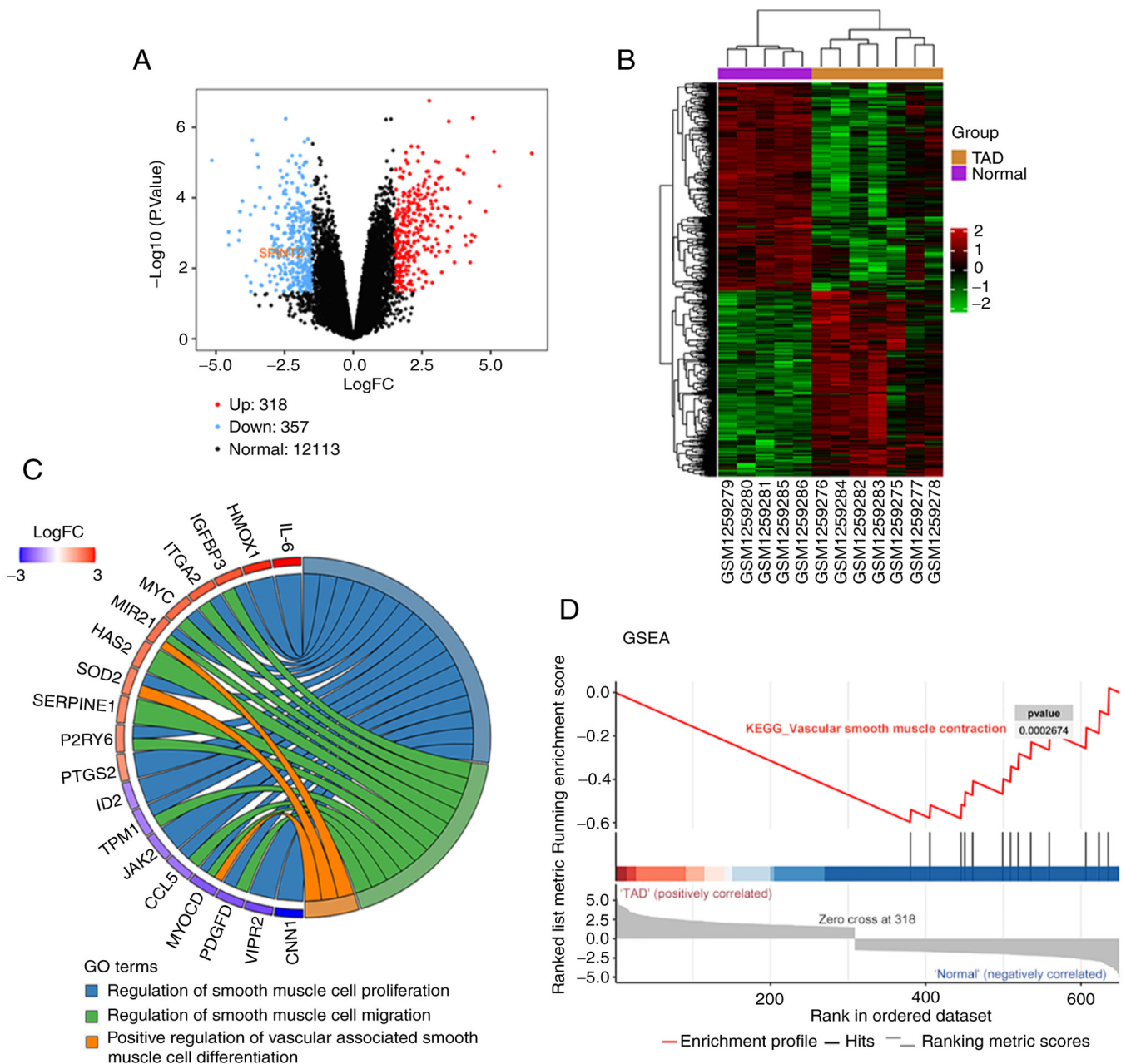


Figure 1. DEG screening of dataset GSE52093 and bioinformatics analysis. (A) Volcano plot of the gene profiles. (B) The gene network was visualized by heatmap, which indicated that the expression of the identified DEGs could correctly distinguish between the TAD and normal samples. (C) Chord plot of GO analysis. (D) GSEA enrichment in the KEGG pathway of vascular smooth muscle contraction (hsa04270). DEG, differentially expressed gene; SPINT2, serine peptidase inhibitor Kunitz type 2; TAD, thoracic aortic dissection; GO, Gene Ontology; GSEA, gene set enrichment analysis; KEGG, Kyoto Encyclopedia of Genes and Genomes.

were used to evaluate the contents of MMP-2 and MMP-9, respectively according to the manufacturer's instructions.

**IF staining.** The sections (5  $\mu\text{m}$ ) of the TAD specimens were incubated overnight at 4°C with the following goat anti-mouse primary antibodies: SPINT2 (1:50; cat. no. sc-398119; Santa Cruz Biotechnology, Inc.) and  $\alpha$ -SMA (1:200; cat. no. AF1032; Affinity Biosciences). Subsequently, they were incubated with fluorescein isothiocyanate (FITC)-labeled goat anti-mouse IgG (1:200; cat. no. ab6785; Abcam) and Cy3-labeled goat anti-rabbit IgG (1:200; cat. no. ab6939; Abcam) secondary antibodies, respectively, for 90 min at room temperature. SMCs were fixed in 4% paraformaldehyde for 15 min at

room temperature and permeabilized with 0.1% Triton X-100 (Beyotime Institute of Biotechnology). Subsequently, the cells were blocked in 1% BSA (Sangon Biotech Co., Ltd.) at room temperature for 15 min and incubated with the following diluted primary antibodies:  $\alpha$ -SMA (1:200; cat. no. AF1032; Affinity Biosciences), SM22 $\alpha$  (1:100; cat. no. AF9266; Affinity Biosciences), Ki-67 (1:100; cat. no. AF0198; Affinity Biosciences) and vimentin (1:200; cat. no. AF7013; Affinity Biosciences) overnight at 4°C. Subsequently, the samples were incubated with the secondary antibody, FITC-labeled goat anti-rabbit IgG (1:200; cat. no. ab6717; Abcam), at room temperature for 60 min. 4',6-diamidino-2-phenylindole (Shanghai Aladdin Biochemical Technology Co., Ltd.) was

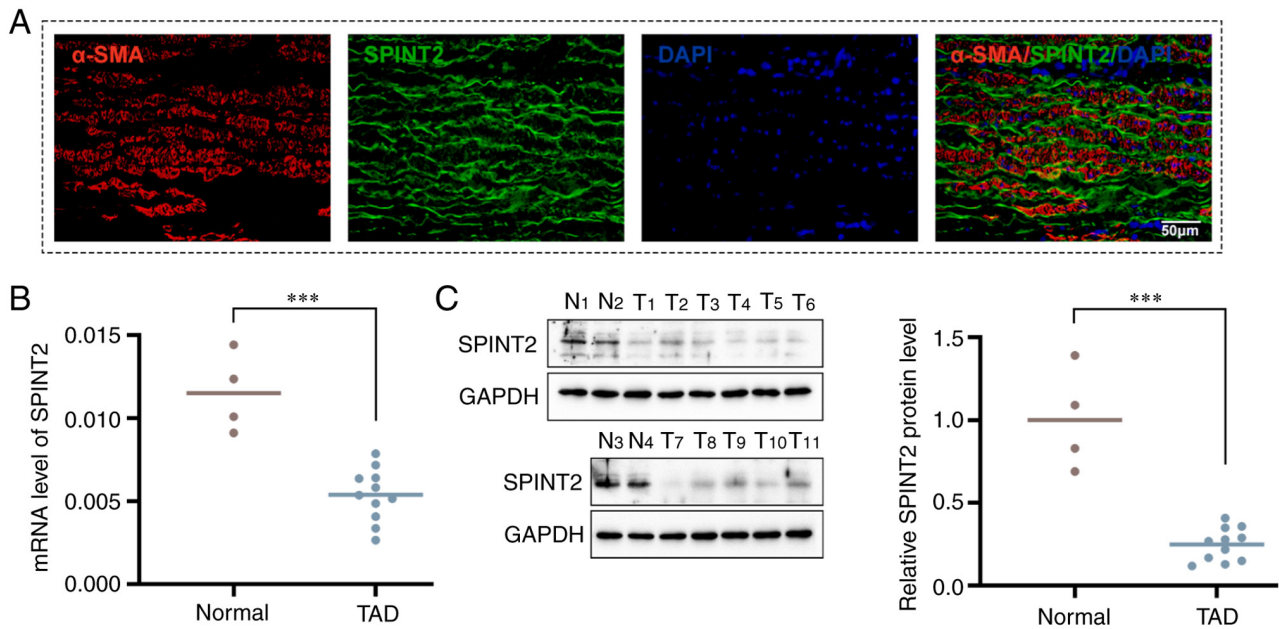


Figure 2. SPINT2 is expressed at low levels in aorta tissues of TAD specimens. (A) SPINT2 expression was co-stained with  $\alpha$ -SMA expression in human TAD specimens. (B) The mRNA levels of SPINT2 in aorta tissues of patients with TAD were determined using reverse transcription-quantitative PCR. (C) SPINT2 protein levels of aorta tissues were analyzed by western blotting. \*\*\* $P < 0.001$  compared with the normal group. SPINT2, serine peptidase inhibitor Kunitz type 2; TAD, thoracic aortic dissection;  $\alpha$ -SMA,  $\alpha$ -small nuclear actin; N, normal group; T, TAD group; DAPI, 4',6-diamidino-2-phenylindole.

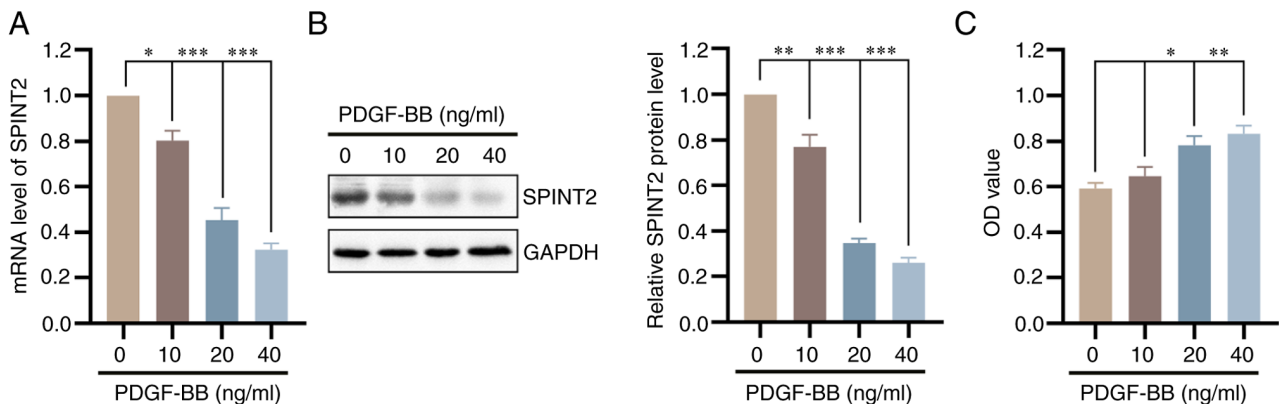


Figure 3. SPINT2 expression is decreased in PDGF-BB-cultured SMCs. SMCs were treated with different concentrations of PDGF-BB (0, 10, 20 and 40 ng/ml) for 24 h. (A and B) The mRNA and protein levels of SPINT2 were measured using reverse transcription-quantitative PCR and western blotting analyses. (C) SMC proliferation was detected using a 3-(4,5-dimethylthiazol-2-yl)-2,5-diphenyltetrazolium bromide assay. \* $P < 0.05$ , \*\* $P < 0.01$  and \*\*\* $P < 0.001$  compared with 0 ng/ml PDGF-BB group. SPINT2, serine peptidase inhibitor Kunitz type 2; PDGF-BB, platelet-derived growth factor BB; SMCs, smooth muscle cells.

used to counterstain the nuclei at room temperature for 5 min. The images were observed under a fluorescence microscope (Olympus Corporation) and imaged at x200 magnification.

**Statistical analysis.** GraphPad Prism 8 software (GraphPad Software; Dotmatics) was used for statistical analysis. All experiments were repeated at least three times. Quantitative values are presented as the mean  $\pm$  standard deviation (SD). Comparisons between two groups were evaluated using unpaired Student's t-test. The comparisons of statistical significance among multiple groups were assessed using one-way analysis of variance, with Tukey's multiple comparison test as the post-hoc analysis.  $P < 0.05$  was considered to indicate a statistically significant difference. All experiments were repeated at least three times.

## Results

*SPINT2 expression is downregulated in TAD, and SMC proliferation, migration and differentiation are related to TAD progression.* A total of 318 upregulated genes (red dots) and 357 downregulated genes (blue dots) were identified from the GSE52093 dataset in ascending aorta samples from patients with TAD compared with the tissues derived from patients devoid of TAD. The differentially expressed SPINT2 was prominently decreased in TAD (Fig. 1A and B). In the GO chord plot, the top 19 GO terms of DEGs indicated that several biological processes, including 'regulation of smooth muscle cell proliferation', 'regulation of smooth muscle cell migration' and 'positive regulation of vascular associated smooth muscle cell differentiation' were enriched in TAD

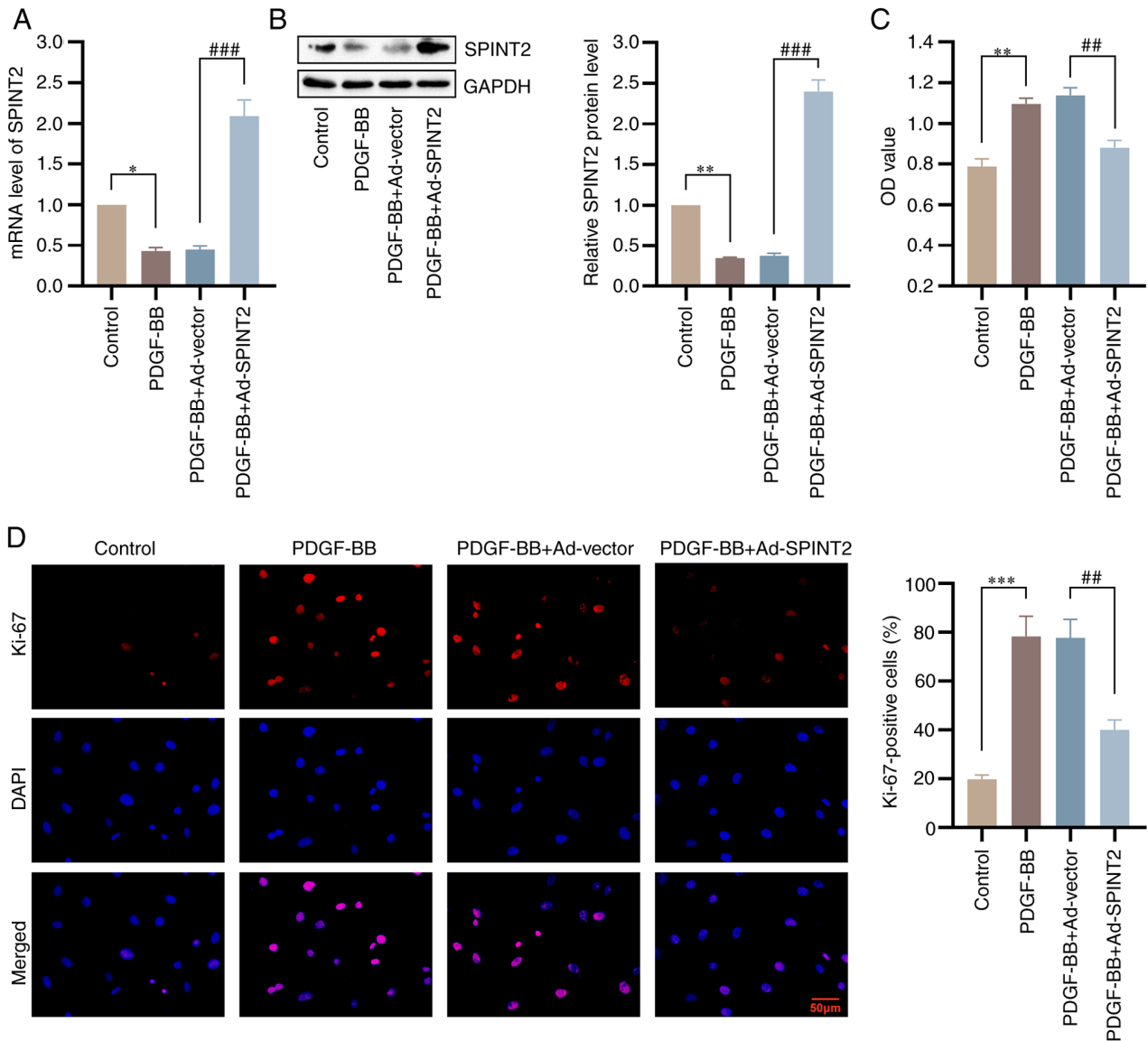


Figure 4. Overexpression of SPINT2 suppresses viability and proliferation of PDGF-BB-treated SMCs. SMCs were infected with NC or SPINT2-overexpression adenovirus for 24 h and subsequently cultured with 20 ng/ml PDGF-BB for 24 h. (A and B) The mRNA and protein levels of SPINT2 were verified by reverse transcription-quantitative PCR and western blotting following PDGF-BB treatment for 24 h. (C) The SMC viability at 48 h following PDGF-BB treatment was detected using a 3-(4,5-dimethylthiazol-2-yl)-2,5-diphenyltetrazolium bromide assay. (D) The expression levels of Ki-67 were determined by immunofluorescence staining to evaluate the SMC proliferation (scale bar, 50  $\mu$ m). \* $P < 0.05$ , \*\* $P < 0.01$  and \*\*\* $P < 0.001$  compared with control group. ## $P < 0.01$  and ### $P < 0.001$  compared with the PDGF-BB + Ad-vector group. SPINT2, serine peptidase inhibitor Kunitz type 2; PDGF-BB, platelet-derived growth factor BB; SMCs, smooth muscle cells; NC, PDGF-BB + Ad-vector; DAPI, 4',6-diamidino-2-phenylindole; Ad, adenovirus.

(Fig. 1C). The GSEA result also showed the negative value of the enrichment score, which indicated that TAD progression was negatively associated with 'vascular smooth muscle contraction' (Fig. 1D).

*SPINT2 is expressed at low levels in aorta tissues of TAD specimens.* In the present study, the location of SPINT2 was identified in aortic dissection specimens by co-staining with  $\alpha$ -SMA. It was found that SPINT2 was mainly localized in the aortic SMCs (Fig. 2A). The expression levels of SPINT2 mRNA and protein in aortic dissection specimens and normal aorta tissues were measured using RT-qPCR and western blotting analyses, respectively. The results further revealed that SPINT2 expression was significantly lower in TAD tissues than that noted in normal aorta tissues ( $P < 0.001$ ; Fig. 2B and C).

*SPINT2 expression is decreased in PDGF-BB-cultured SMCs.* As shown in Fig. S1, the cells isolated from mice were identified as SMCs by positive  $\alpha$ -SMA and SM22 $\alpha$  staining. Subsequently, SMCs were cultured with different concentrations of PDGF-BB for 24 h and SPINT2 expression was detected. Both the mRNA and protein levels of SPINT2 were significantly decreased following PDGF-BB stimulation in a concentration-dependent manner ( $P < 0.05$ ; Fig. 3A and B). The MTT assay confirmed that the cell viability of SMCs was increased in the presence of PDGF-BB ( $P < 0.05$ ; Fig. 3C).

*Overexpression of SPINT2 suppresses viability and proliferation of PDGF-BB-treated SMCs.* Initially, the SMCs were infected with the adenoviral vector, Ad-SPINT2, to construct SPINT2-overexpressed cell lines. The mRNA and protein

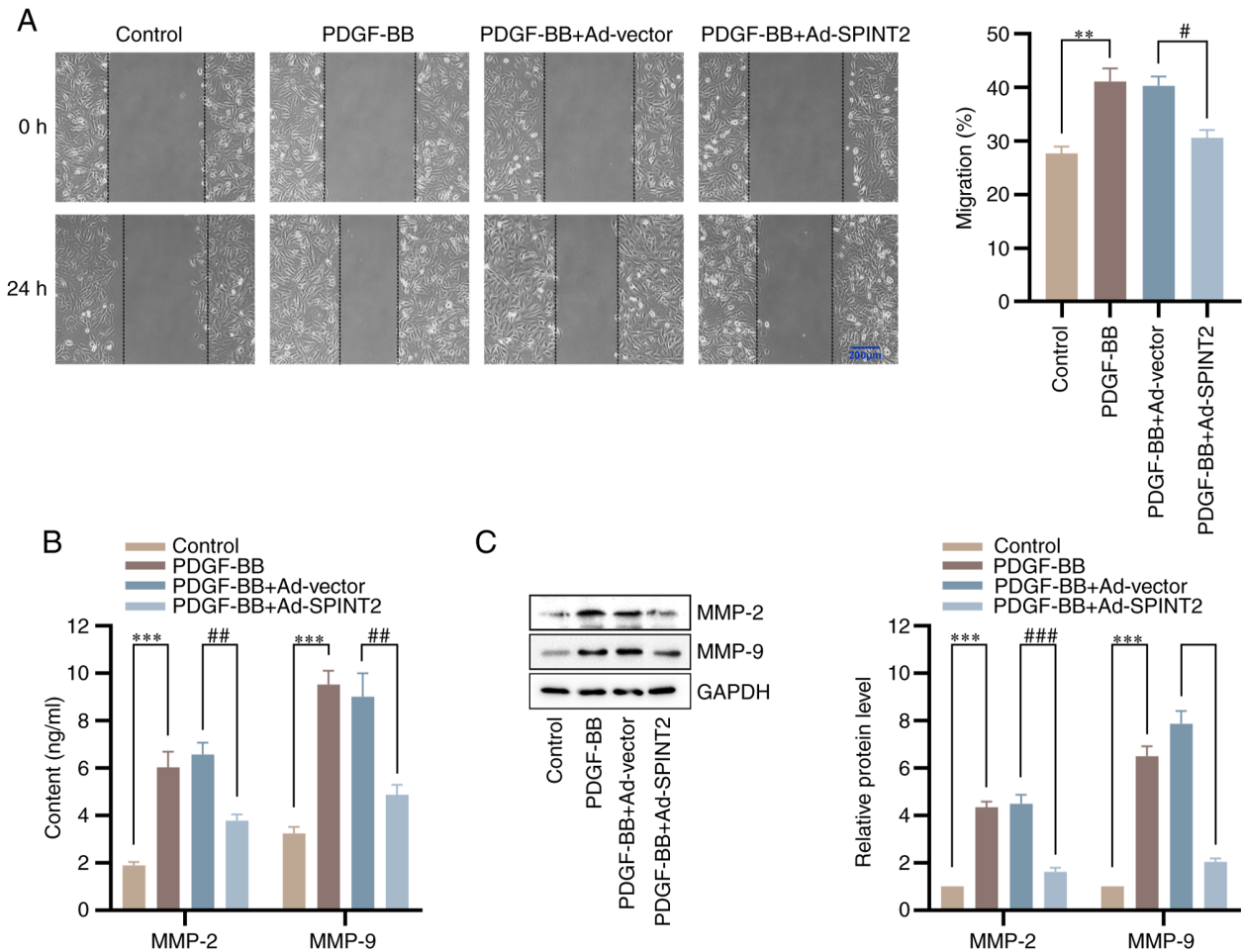


Figure 5. Overexpression of SPINT2 inhibits SMC migration and expression of MMPs. (A) Representative images and quantification of the wound healing assay. Scale bar, 200  $\mu$ m. (B and C) The expression levels of MMP-2 and MMP-9 were determined using ELISA and western blotting. \*\* $P < 0.01$  and \*\*\* $P < 0.001$  compared with the control group. # $P < 0.05$ , ## $P < 0.01$  and ### $P < 0.001$  compared with the PDGF-BB + Ad-vector group. SPINT2, serine peptidase inhibitor Kunitz type 2; SMC, smooth muscle cells; MMP, matrix metalloproteinase; PDGF-BB, platelet-derived growth factor BB; Ad, adenovirus.

expression levels of SPINT2 were significantly increased in the Ad-SPINT2 group compared with those in the control group, which confirmed the successful construction of the adenoviral model overexpressing SPINT2 (Fig. S2). To explore the effect of SPINT2 on SMC viability and phenotypic switching without PDGF-BB, an MTT assay was conducted and the expression levels of SMC synthetic markers (vimentin and collagen I) and contractile markers ( $\alpha$ -SMA and SM22 $\alpha$ ) were measured using western blotting. As shown in Fig. S3, SPINT2 overexpression has no marked effects on SMC viability or phenotypic switching. After treatment with 20 ng/ml PDGF-BB for 24 h, the expression of SPINT2 was markedly increased in SMCs infected with an adenovirus overexpressing SPINT2. The PDGF-BB-induced decrease in SPINT2 was also reversed following infection of the cells with SPINT2 overexpression adenovirus ( $P < 0.001$ ; Fig. 4A and B). PDGF receptor  $\beta$  (PDGFR $\beta$ ) protein levels were determined using western blotting as shown in Fig. S4. PDGFR $\beta$  expression was higher in the presence of PDGF-BB compared with the control group. The PDGF-BB-induced increase in PDGFR $\beta$  was also reversed following infection of the cells with SPINT2 overexpression adenovirus. To investigate the roles of SPINT2 in SMC viability, an MTT assay was conducted, which confirmed that

SPINT2 inhibited the high viability of SMCs in the presence of PDGF-BB (Fig. 4C). SMC proliferation was detected via the presence of Ki-67-positive cells (IF staining). PDGF-BB stimulation increased the number of Ki-67-positive cells. However, SPINT2 overexpression decreased the number of Ki-67-positive cells (Fig. 4D). The data confirmed the inhibitory effects of SPINT2 on SMC viability and proliferation.

*Overexpression of SPINT2 inhibits SMC migration and expression of MMPs.* To explore the effects of SPINT2 on SMC migration, a wound healing assay was conducted. Following stimulation of the cells with PDGF-BB for 24 h, the wound healing was increased, whereas the PDGF-BB-induced SMC migration was reduced by SPINT2 (Fig. 5A). To further determine the mechanisms of the inhibitory effects of SPINT2 on SMC migration, ELISA and western blotting assays were used to measure the content and expression levels of MMP-2 and MMP-9, which are involved in SMC migration via ECM degradation (21). SPINT2 significantly blocked the increase in MMP-2 and MMP-9 content and expression in SMCs induced by PDGF-BB (Fig. 5B and C). These results indicated that SPINT2 exerted inhibitory effects on SMC migration via MMP-2 and MMP-9.

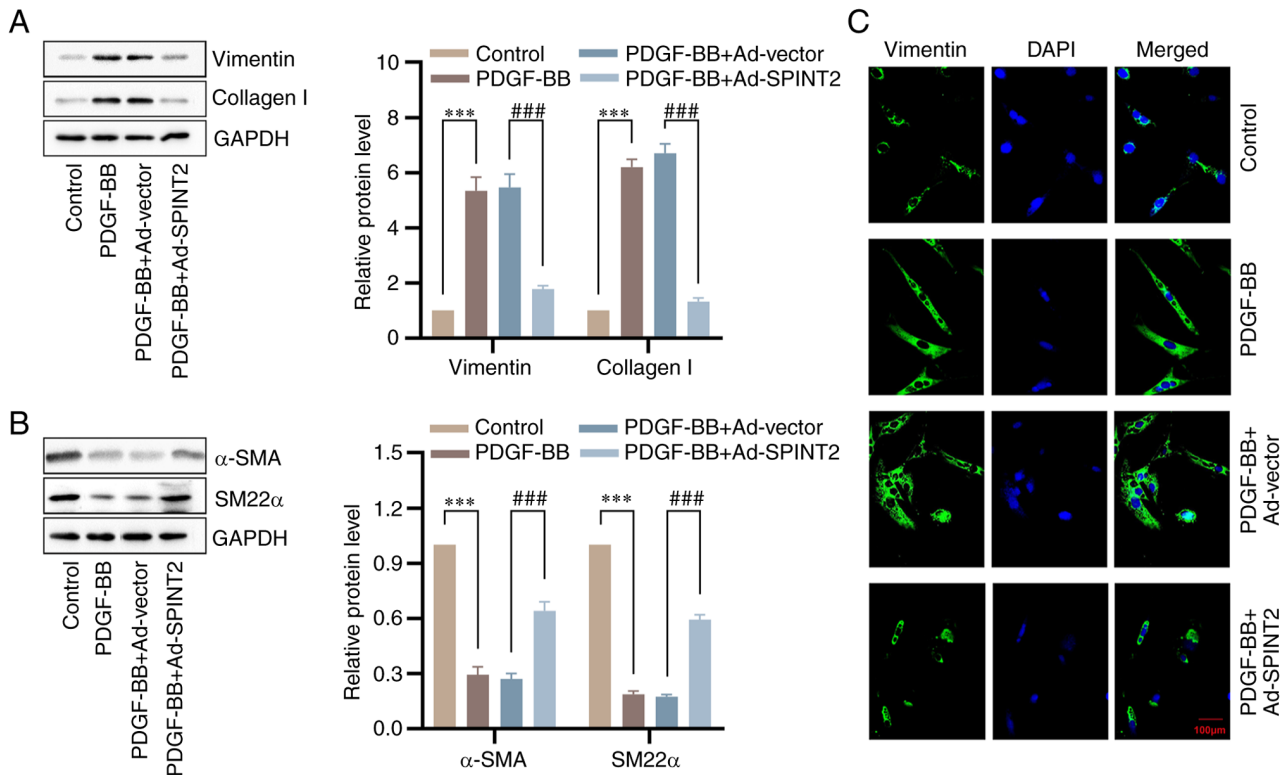


Figure 6. Overexpression of SPINT2 prevents PDGF-BB-induced SMC phenotypic switching. SMCs were incubated with 20 ng/ml PDGF-BB for 24 h following 24 h of adenoviral infection. (A) The expression levels of the synthetic proteins (vimentin and collagen I) were detected by western blotting. (B) The expression levels of the contractile proteins ( $\alpha$ -SMA and SM22 $\alpha$ ) were detected by western blotting. (C) The expression levels of vimentin were assessed by immunofluorescence analysis. The nuclei were stained with DAPI. Scale bar, 100  $\mu$ m. \*\*\* $P$ <0.001 compared with the control group. ### $P$ <0.001 compared with the PDGF-BB + Ad-vector group. SPINT2, serine peptidase inhibitor Kunitz type 2; PDGF-BB, platelet-derived growth factor BB; SMCs, smooth muscle cells;  $\alpha$ -SMA, smooth muscle  $\alpha$ -actin; SM22 $\alpha$ , smooth muscle protein 22- $\alpha$ ; DAPI, 4',6-diamidino-2-phenylindole; Ad, adenovirus.

*Overexpression of SPINT2 prevents PDGF-BB-induced SMC phenotypic switching.* To confirm the effects of SPINT2 on SMC phenotypic switching, the expression levels of vimentin, collagen I,  $\alpha$ -SMA and SM22 $\alpha$  were measured using western blotting. The results indicated that PDGF-BB treatment resulted in a significant upregulation in the protein levels of vimentin and collagen I, and a downregulation in the protein levels of  $\alpha$ -SMA and SM22 $\alpha$ . However, the promotional effects of PDGF-BB on the synthetic markers and the inhibitory effects on the contractile markers were mitigated by SPINT2 overexpression (Fig. 6A and B). Meanwhile, the IF assay demonstrated a similarly altered trend for vimentin in SMCs (Fig. 6C).

*SPINT2 reverses SMC phenotypic switching induced by the activation of the ERK pathway.* To further explore the mechanism by which SPINT2 regulates SMC phenotypic switching, the present study focused on the effect of SPINT2 overexpression on the activation of ERK. Western blotting analysis indicated that SPINT2 markedly inhibited the PDGF-BB-induced increase in p-ERK protein in SMCs, whereas the expression of ERK was not significantly different before or after PDGF-BB treatment (Fig. 7A). Administration of TPA (an ERK agonist) attenuated the SPINT2-mediated inhibition of viability in PDGF-BB-treated SMCs (Fig. 7B). In addition, TPA markedly reversed downregulation of MMP-2 and MMP-9 contents induced by SPINT2 (Fig. 7C). Furthermore, TPA significantly blocked the SPINT2-mediated

decrease in the level of vimentin and the increase in the levels of SM22 $\alpha$  in PDGF-BB-treated SMCs (Fig. 7D and E).

## Discussion

SMCs are the major cellular component of the aortic wall, and their dysregulation can disturb aortic function and homeostasis, leading to TAD pathogenesis (22). The results of the present study revealed a significant decrease in SPINT2 expression in the aorta tissues of patients with TAD and in PDGF-BB-induced SMCs, suggesting that SPINT2 may be related to the development of TAD. Furthermore, SPINT2 overexpression suppressed PDGF-BB-induced SMC proliferation, migration and MMP production, and prevented synthetic phenotype switching of PDGF-BB-induced SMCs via ERK activation.

The principal function of SMCs in the body is to regulate blood flow through the contraction and relaxation of the vessel walls (23). In response to environmental stress, SMCs undergo phenotype switching from a differentiated and quiescent 'contractile' state to a highly proliferative and migratory 'synthetic' state, which is considered as a major driver in the pathogenesis of TAD (24). It has been demonstrated that PDGF-BB is a potent stimulant of SMC proliferation and migration (25). Both *in vitro* and *in vivo* results indicated that inhibition of SMC proliferation and migration by downregulation of SPINT2 expression may suppress vascular-media degeneration and mitigate the loss of elastic-fiber integrity

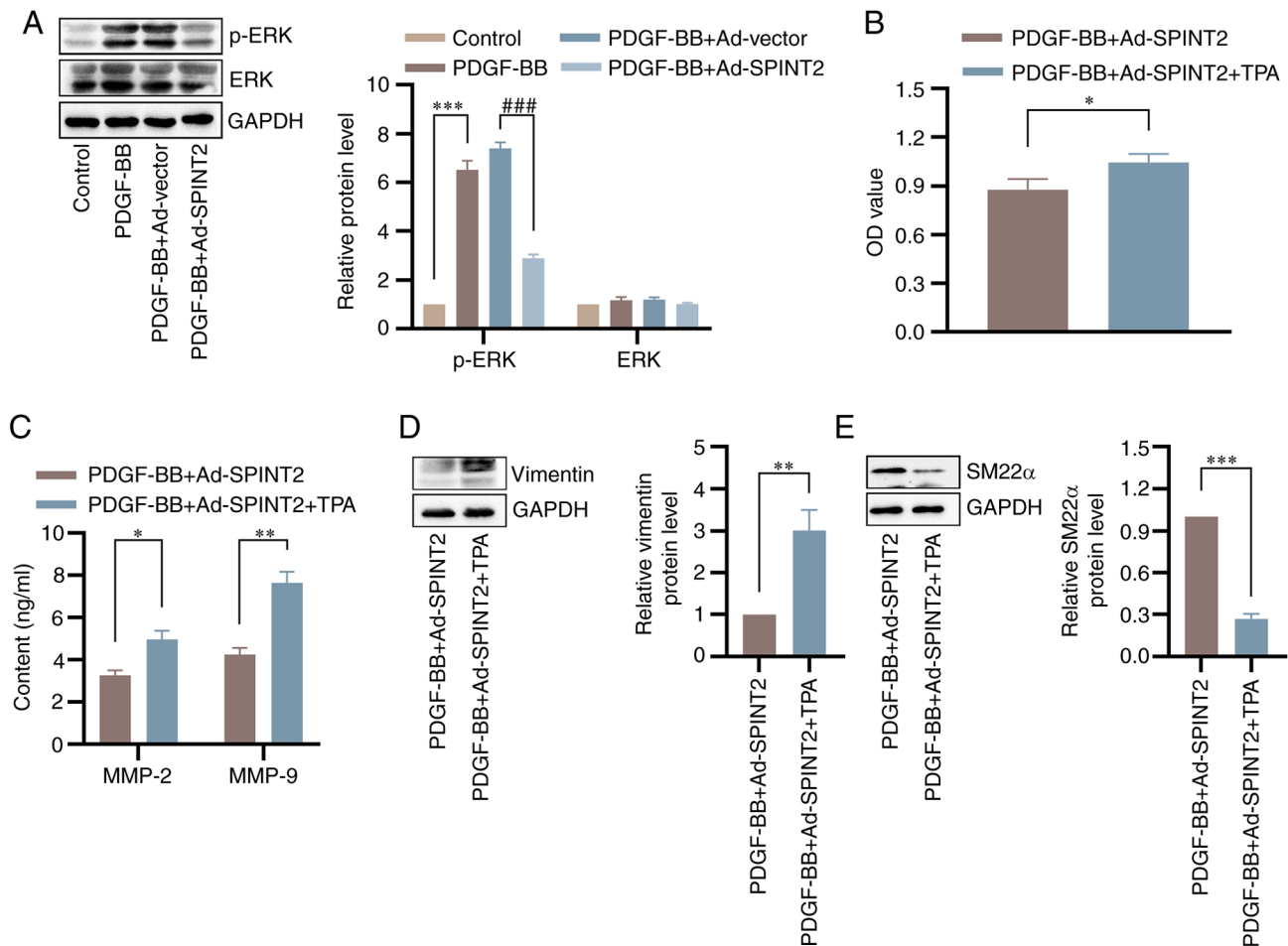


Figure 7. SPINT2 regulates SMC phenotypic transition via activation of the ERK signaling pathway. (A) SMCs were incubated with 20 ng/ml PDGF-BB for 24 h following 24 h of adenoviral infection. The expression levels of p-ERK and ERK in SMCs were detected by western blotting. \*\*\* $P < 0.001$  compared with the control group. ### $P < 0.001$  compared with the PDGF-BB + Ad-vector group. (B) SMCs were cultured with 100 nmol/l TPA following 24 h of adenoviral infection. SMC proliferation at 48 h following PDGF-BB treatment was detected using a 3-(4,5-dimethylthiazol-2-yl)-2,5-diphenyltetrazolium bromide assay. (C) Following 24 h of PDGF-BB treatment, the expression levels of MMP-2 and MMP-9 were determined using ELISA. (D and E) The expression levels of vimentin and SM22 $\alpha$  proteins were detected by western blotting. \* $P < 0.05$ , \*\* $P < 0.01$  and \*\*\* $P < 0.001$  compared with the PDGF-BB + Ad-SPINT2 group. SPINT2, serine peptidase inhibitor Kunitz type 2; SMCs, smooth muscle cells; PDGF-BB, platelet-derived growth factor BB; p, phosphorylated; TPA, tetradecanoylphorbol-13-acetate; MMP, matrix metalloproteinase; SM22 $\alpha$ , smooth muscle protein 22- $\alpha$ ; Ad, adenovirus.

in TAD (26). However, to the best of our knowledge the role of SPINT2 in SMC proliferation and migration has not been investigated to date. It was reported that SPINT2 could inhibit cell proliferation and migration in diverse cancer cell lines (27). For example, in a breast cancer cell line, the elimination of SPINT2 expression significantly enhanced the proliferative and invasive nature of the cells (28). Moreover, SPINT2 could inhibit cell proliferation, migration and invasion in endometrial cancer (EC) cell lines. Therefore, it may be considered as a therapeutic target and a favorable prognostic marker for EC (18). Furthermore, SPINT2 suppressed the cellular invasion and metastasis of prostate cancer via inhibition of transmembrane protease serine 2 expression (15) and regulation of matriptase (29). One study verified that decreased SPINT2 expression was significantly associated with tumor invasion, metastasis and poor prognosis in patients with non-small cell lung cancer (30). In lung cancer cells, SPINT2 repressed cell motility and metastasis as a novel inhibitor of plasmin (31). In line with previous reports, the results of the present study suggested that SPINT2 suppressed PDGF-BB-induced SMC viability and migration *in vitro*.

ECM degradation is mainly regarded as a key pathophysiological feature in TAD formation (32). MMP-2 and MMP-9, which belong to the MMP family, are important in ECM remodeling (33,34). In the present study, significantly increased expression levels of MMP-2 and MMP-9 were noted in SMCs of aorta tissues from patients with TAD, suggesting that MMP-2 and MMP-9 promote degradation of proteins associated with fibrosis and causing vulnerability of aorta via hemodynamic stress, which is involved in TAD formation. Previous studies verified that PDGF-BB markedly upregulated the expression levels of MMP-2 and MMP-9 in SMCs (35,36). By contrast, it was shown that SPINT2 could downregulate MMP-2 expression in high-grade glioma cell lines (17). In the present study, the results demonstrated that the expression levels of SPINT2 were associated negatively with those of MMP-2 and MMP-9 in PDGF-BB-induced SMCs, suggesting that administration of SPINT2 may alleviate TAD-stimulated ECM remodeling and prevent the formation of TAD via downregulation of MMP-2 and MMP-9 expression in aortic SMCs.

In TAD progression, SMCs usually present with a prevalent synthetic phenotype as opposed to a contractile

phenotype, causing an impaired contractile function and endothelial-dependent relaxation of the aortic tissue (37,38). It was previously reported that SMCs decreased the expression levels of contractile/differentiated markers,  $\alpha$ -SMA and SM22 $\alpha$ , under a synthetic state (39), along with an increase in the expression levels of the synthetic/dedifferentiated marker, vimentin (40). PDGF-BB is essential for inducing a dedifferentiated state of SMCs (41), and the inhibitory effects of SPINT2 on vimentin expression have been verified (18). However, the significance of SPINT2 in the regulation of SMC phenotypic switching requires further elucidation and thus, the potential effect of SPINT2 on phenotype switching of SMCs was further studied *in vitro* in the present study. Initially, it was found that PDGF-BB promoted SMC dedifferentiation by conversion from a contractile to a synthetic state, which was consistent with previous studies (42,43). Moreover, SPINT2 blocked PDGF-BB-induced SMC dedifferentiation by increasing the levels of the contractile proteins and decreasing the levels of the synthetic markers, indicating that it participated in the maintenance of SMC contractility.

There is extensive crosstalk of the HGF/MET axis with numerous other signaling pathways, including growth factor-dependent pathways (such as PI3K/AKT/mTOR and RAS/RAF/ERK) (44). ERK signaling has been implicated as a driver of aortic aneurysm pathogenesis by mediating contractile-to-synthetic phenotype switching of SMCs (45). For example, Liang *et al.* (46) indicated that berberine blocked injury-induced SMC regrowth *in vitro* via inactivation of the ERK signaling pathway. In addition, IL-11 caused SMC phenotypic switching to a similar extent with TGF $\beta$ 1 or angiotensin II stimulation, via activation of ERK signaling, which played an important role in aortic pathobiology (47). It had been reported that increased cell motility that was associated with SPINT2 silencing was abrogated by treatment with ERK/MAPK inhibitors (10). Therefore, ERK as a MET-downstream signal was investigated in the present study. However, whether ERK is involved in the regulation of SPINT2 for SMC phenotypic switching remains unknown. TPA acts as an activator of the ERK/MAPK signaling pathway. In transgenic (Eisuke) mice expressing ERK fluorescence resonance energy transfer biosensors, treatment with TPA resulted in a gradual increase in ERK activity, peaking at ~6 h (48). In A549 cells, a human lung cancer cell line, TPA served as a potent ERK activator that was observed to induce early, intense and relatively transient phosphorylation of ERK (49). In mouse dual specificity phosphatase 5(+/-) embryonic fibroblasts, the application of TPA led to an elevation in ERK expression levels (50). MMP-9 secretion induced by PDGF/IL-1 was mediated via the ERK pathway, which was induced by TPA specifically (51). Therefore, TPA was selected as an ERK agonist to explore the effects of SPINT2 overexpression on ERK activation in the present study. The results of the present study demonstrated that the expression of p-ERK was downregulated by SPINT2. Activation of ERK using TPA partially abolished the SPINT2-mediated inhibitory effect on SMC proliferation and dedifferentiation. Therefore, it was suggested that SPINT2 reversed SMC phenotypic switching induced by activation of the ERK pathway.

The present study reported that SPINT2 levels were significantly downregulated in the aorta tissues of patients with TAD and that SPINT2 overexpression in a mouse vascular SMC line could inhibit cell proliferation and migration, MMP-2 and MMP-9 expression, and phenotypic switching from a contractile to a synthetic type. These findings indicate that SPINT2 protects against TAD development. However, the present study had several limitations that should be mentioned. Control aortic specimens obtained from patients devoid of TAD were used only for RT-qPCR and western blotting. Therefore, SPINT2 expression levels in dissection vs. control tissues were not compared by IF or IHC images. In future studies, if suitable samples are encountered, they will be collected and IF or IHC staining will be used to detect the SPINT2 expression levels in TAD lesions more intuitively. In addition, conclusions were drawn from cell experiments only, and it is crucial to verify the role of SPINT2 in TAD formation in animal experiments. *In vivo* experiments will be performed in future studies.

### Acknowledgements

Not applicable.

### Funding

No funding was received.

### Availability of data and materials

The datasets used and/or analyzed during the current study are available from the corresponding author on reasonable request.

### Authors' contributions

CY conceived the project, designed the experiments and revised the paper. JL performed the experiments and wrote the original paper. KY, ZC, DX, BZ, WX and HO assisted with the experiments, data analysis and interpretation. All authors read and approved the final version of the manuscript. CY and JL confirm the authenticity of all the raw data.

### Ethics approval and consent to participate

This study was approved by The Medical Ethics Committee of the First Affiliated Hospital of Anhui Medical University (Hefei, China; approval no. Quick-PJ 2022-14-49). The animal experimental procedures were performed with the approval of The Experimental Animal Ethics Committee of Anhui Medical University (Hefei, China; approval no. LLSC20220940). Written informed consent regarding the use of specimens was obtained from all patients prior to participation in the study.

### Patient consent for publication

Not applicable.

### Competing interests

The authors declare that they have no competing interests.

## References

- Xu Y, Ye J, Wang M, Wang Y, Ji Q, Huang Y, Zeng T, Wang Z, Ye D, Jiang H, *et al*: Increased interleukin-11 levels in thoracic aorta and plasma from patients with acute thoracic aortic dissection. *Clin Chim Acta* 481: 193-199, 2018.
- DeMartino RR, Sen I, Huang Y, Bower TC, Oderich GS, Pochettino A, Greason K, Kalra M, Johnstone J, Shuja F, *et al*: Population-based assessment of the incidence of aortic dissection, intramural hematoma, and penetrating ulcer, and its associated mortality from 1995 to 2015. *Circ Cardiovasc Qual Outcomes* 11: e004689, 2018.
- Doyle BJ and Norman PE: Computational biomechanics in thoracic aortic dissection: Today's approaches and Tomorrow's opportunities. *Ann Biomed Eng* 44: 71-83, 2016.
- Fukui T: Management of acute aortic dissection and thoracic aortic rupture. *J Intensive Care* 6: 15, 2018.
- Rombouts KB, van Merriënboer TAR, Ket JCF, Bogunovic N, van der Velden J and Yeung KK: The role of vascular smooth muscle cells in the development of aortic aneurysms and dissections. *Eur J Clin Invest* 52: e13697, 2022.
- Yuan Y, Wang C, Xu J, Tao J, Xu Z and Huang S: BRG1 overexpression in smooth muscle cells promotes the development of thoracic aortic dissection. *BMC Cardiovasc Disord* 14: 144, 2014.
- Rodrigues Bento J, Meester J, Luyckx I, Peeters S, Verstraeten A and Loeys B: The genetics and typical traits of thoracic aortic aneurysm and dissection. *Annu Rev Genomics Hum Genet* 23: 223-253, 2022.
- Zhang X, Shen YH and LeMaire SA: Thoracic aortic dissection: Are matrix metalloproteinases involved? *Vascular* 17: 147-157, 2009.
- Li T, Lv Z, Jing JJ, Yang J and Yuan Y: Matrix metalloproteinase family polymorphisms and the risk of aortic aneurysmal diseases: A systematic review and meta-analysis. *Clin Genet* 93: 15-32, 2018.
- Morris MR, Gentle D, Abdulrahman M, Maina EN, Gupta K, Banks RE, Wiesener MS, Kishida T, Yao M, Teh B, *et al*: Tumor suppressor activity and epigenetic inactivation of hepatocyte growth factor activator inhibitor type 2/SPINT2 in papillary and clear cell renal cell carcinoma. *Cancer Res* 65: 4598-4606, 2005.
- Kawaguchi T, Qin L, Shimomura T, Kondo J, Matsumoto K, Denda K and Kitamura N: Purification and cloning of hepatocyte growth factor activator inhibitor type 2, a Kunitz-type serine protease inhibitor. *J Biol Chem* 272: 27558-27564, 1997.
- Rosen EM, Lamszus K, Laterra J, Polverini PJ, Rubin JS and Goldberg ID: HGF/SF in angiogenesis. *Ciba Found Symp* 212: 215-229, 1997.
- Gallo S, Sala V, Gatti S and Crepaldi T: Cellular and molecular mechanisms of HGF/Met in the cardiovascular system. *Clin Sci (Lond)* 129: 1173-1193, 2015.
- Kawaguchi M and Kataoka H: Mechanisms of hepatocyte growth factor activation in cancer tissues. *Cancers (Basel)* 6: 1890-1904, 2014.
- Ko CJ, Hsu TW, Wu SR, Lan SW, Hsiao TF, Lin HY, Lin HH, Tu HF, Lee CF, Huang CC, *et al*: Inhibition of TMPRSS2 by HAI-2 reduces prostate cancer cell invasion and metastasis. *Oncogene* 39: 5950-5963, 2020.
- Nakamura K, Abarzua F, Hongo A, Kodama J, Nasu Y, Kumon H and Hiramatsu Y: Hepatocyte growth factor activator inhibitors (HAI-1 and HAI-2) are potential targets in uterine leiomyosarcoma. *Int J Oncol* 37: 605-614, 2010.
- Pereira MS, Celeiro SP, Costa AM, Pinto F, Popov S, de Almeida GC, Amorim J, Pires MM, Pinheiro C, Lopes JM, *et al*: Loss of SPINT2 expression frequently occurs in glioma, leading to increased growth and invasion via MMP2. *Cell Oncol (Dordr)* 43: 107-121, 2020.
- Nakamura K, Hongo A, Kodama J and Hiramatsu Y: The role of hepatocyte growth factor activator inhibitor (HAI)-1 and HAI-2 in endometrial cancer. *Int J Cancer* 128: 2613-2624, 2011.
- Golovina VA and Blaustein MP: Preparation of primary cultured mesenteric artery smooth muscle cells for fluorescent imaging and physiological studies. *Nat Protoc* 1: 2681-2687, 2006.
- Livak KJ and Schmittgen TD: Analysis of relative gene expression data using real-time quantitative PCR and the 2(-Delta Delta C(T)) method. *Methods* 25: 402-408, 2001.
- Zhu N, Xiang Y, Zhao X, Cai C, Chen H, Jiang W, Wang Y and Zeng C: Thymoquinone suppresses platelet-derived growth factor-BB-induced vascular smooth muscle cell proliferation, migration and neointimal formation. *J Cell Mol Med* 23: 8482-8492, 2019.
- Shen YH, LeMaire SA, Webb NR, Cassis LA, Daugherty A and Lu HS: Aortic aneurysms and dissections series. *Arterioscler Thromb Vasc Biol* 40: e37-e46, 2020.
- Liu R, Leslie KL and Martin KA: Epigenetic regulation of smooth muscle cell plasticity. *Biochim Biophys Acta* 1849: 448-453, 2015.
- Grond-Ginsbach C, Pjontek R, Aksay SS, Hyhlik-Durr A, Bockler D and Gross-Weissmann ML: Spontaneous arterial dissection: Phenotype and molecular pathogenesis. *Cell Mol Life Sci* 67: 1799-1815, 2010.
- Bornfeldt KE, Raines EW, Graves LM, Skinner MP, Krebs EG and Ross R: Platelet-derived growth factor. Distinct signal transduction pathways associated with migration versus proliferation. *Ann N Y Acad Sci* 766: 416-430, 1995.
- Sun L, Wang C, Yuan Y, Guo Z, He Y, Ma W and Zhang J: Downregulation of HDAC1 suppresses media degeneration by inhibiting the migration and phenotypic switch of aortic vascular smooth muscle cells in aortic dissection. *J Cell Physiol* 235: 8747-8756, 2020.
- Roversi FM, Olalla Saad ST and Machado-Neto JA: Serine peptidase inhibitor Kunitz type 2 (SPINT2) in cancer development and progression. *Biomed Pharmacother* 101: 278-286, 2018.
- Parr C and Jiang WG: Hepatocyte growth factor activation inhibitors (HAI-1 and HAI-2) regulate HGF-induced invasion of human breast cancer cells. *Int J Cancer* 119: 1176-1183, 2006.
- Tsai CH, Teng CH, Tu YT, Cheng TS, Wu SR, Ko CJ, Shyu HY, Lan SW, Huang HP, Tzeng SF, *et al*: HAI-2 suppresses the invasive growth and metastasis of prostate cancer through regulation of matriptase. *Oncogene* 33: 4643-4652, 2014.
- Ma Z, Liu D, Li W, Di S, Zhang Z, Zhang J, Xu L, Guo K, Zhu Y, Han J, *et al*: STYK1 promotes tumor growth and metastasis by reducing SPINT2/HAI-2 expression in non-small cell lung cancer. *Cell Death Dis* 10: 435, 2019.
- Wu SR, Lin CH, Shih HP, Ko CJ, Lin HY, Lan SW, Lin HH, Tu HF, Ho CC, Huang HP and Lee MS: HAI-2 as a novel inhibitor of plasmin represses lung cancer cell invasion and metastasis. *Br J Cancer* 120: 499-511, 2019.
- Maguire EM, Pearce SWA, Xiao R, Oo AY and Xiao Q: Matrix metalloproteinase in abdominal aortic aneurysm and aortic dissection. *Pharmaceuticals (Basel)* 12: 118, 2019.
- Liu O, Li J, Xin Y, Qin Y, Li H, Gong M, Liu Y, Wang X, Li J and Zhang H: Association of MMP-2 gene haplotypes with thoracic aortic dissection in Chinese Han population. *BMC Cardiovasc Disord* 16: 11, 2016.
- Huang H: Matrix Metalloproteinase-9 (MMP-9) as a cancer biomarker and MMP-9 biosensors: Recent advances. *Sensors (Basel)* 18: 3249, 2018.
- Hsuan CF, Lu YC, Tsai IT, Hwang JY, Wang SW, Chang TH, Chen YL and Chang CC: *Glossogyne tenuifolia* Attenuates proliferation and migration of vascular smooth muscle cells. *Molecules* 25: 5825, 2020.
- Jing Y, Gao B, Han Z, Xia L and Xin S: The protective effect of HOXA5 on carotid atherosclerosis occurs by modulating the vascular smooth muscle cell phenotype. *Mol Cell Endocrinol* 534: 111366, 2021.
- Romaniello F, Mazzaglia D, Pellegrino A, Grego S, Fiorito R, Ferlosio A, Chiariello L and Orlandi A: Aortopathy in Marfan syndrome: An update. *Cardiovasc Pathol* 23: 261-266, 2014.
- Milewicz DM, Trybus KM, Guo DC, Sweeney HL, Regalado E, Kamm K and Stull JT: Altered smooth muscle cell force generation as a driver of thoracic aortic aneurysms and dissections. *Arterioscler Thromb Vasc Biol* 37: 26-34, 2017.
- Zhu SB, Zhu J, Zhou ZZ, Xi EP, Wang RP and Zhang Y: TGF-β1 induces human aortic vascular smooth muscle cell phenotype switch through PI3K/AKT/ID2 signaling. *Am J Transl Res* 7: 2764-2774, 2015.
- Shi X, Ma W, Pan Y, Li Y, Wang H, Pan S, Tian Y, Xu C and Li L: MiR-126-5p promotes contractile switching of aortic smooth muscle cells by targeting VEPH1 and alleviates Ang II-induced abdominal aortic aneurysm in mice. *Lab Invest* 100: 1564-1574, 2020.
- Kim S and Kang H: miR-15b induced by platelet-derived growth factor signaling is required for vascular smooth muscle cell proliferation. *BMB Rep* 46: 550-554, 2013.
- Shi N, Li CX, Cui XB, Tomarev SI and Chen SY: Olfactomedin 2 regulates smooth muscle phenotypic modulation and vascular remodeling through mediating runt-related transcription factor 2 binding to serum response factor. *Arterioscler Thromb Vasc Biol* 37: 446-454, 2017.

43. Liu H, Chen H, Deng X, Peng Y, Zeng Q, Song Z, He W, Zhang L, Xiao T, Gao G and Li B: Knockdown of TRIM28 inhibits PDGF-BB-induced vascular smooth muscle cell proliferation and migration. *Chem Biol Interact* 311: 108772, 2019.
44. Fasolo A, Sessa C, Gianni L and Broggin M: Seminars in clinical pharmacology: An introduction to MET inhibitors for the medical oncologist. *Ann Oncol* 24: 14-20, 2013.
45. Pedroza AJ, Koyano T, Trojan J, Rubin A, Palmon I, Jaatinen K, Burdon G, Chang P, Tashima Y, Cui JZ, *et al*: Divergent effects of canonical and non-canonical TGF- $\beta$  signalling on mixed contractile-synthetic smooth muscle cell phenotype in human Marfan syndrome aortic root aneurysms. *J Cell Mol Med* 24: 2369-2383, 2020.
46. Liang KW, Ting CT, Yin SC, Chen YT, Lin SJ, Liao JK and Hsu SL: Berberine suppresses MEK/ERK-dependent Egr-1 signaling pathway and inhibits vascular smooth muscle cell regrowth after in vitro mechanical injury. *Biochem Pharmacol* 71: 806-817, 2006.
47. Lim WW, Corden B, Ng B, Vanezis K, D'Agostino G, Widjaja AA, Song WH, Xie C, Su L, Kwek XY, *et al*: Interleukin-11 is important for vascular smooth muscle phenotypic switching and aortic inflammation, fibrosis and remodeling in mouse models. *Sci Rep* 10: 17853, 2020.
48. Hiratsuka T, Fujita Y, Naoki H, Aoki K, Kamioka Y and Matsuda M: Intercellular propagation of extracellular signal-regulated kinase activation revealed by in vivo imaging of mouse skin. *Elife* 4: e05178, 2015.
49. Refsnes M, Skuland T, Lag M, Schwarze PE and Ovrevik J: Differential NF-kappaB and MAPK activation underlies fluoride- and TPA-mediated CXCL8 (IL-8) induction in lung epithelial cells. *J Inflamm Res* 7: 169-185, 2014.
50. Rushworth LK, Kidger AM, Delavaine L, Stewart G, van Schelven S, Davidson J, Bryant CJ, Caddy E, East P, Caunt CJ and Keyse SM: Dual-specificity phosphatase 5 regulates nuclear ERK activity and suppresses skin cancer by inhibiting mutant Harvey-Ras (HRasQ61L)-driven SerpinB2 expression. *Proc Natl Acad Sci USA* 111: 18267-18272, 2014.
51. Turner NA, O'Regan DJ, Ball SG and Porter KE: Simvastatin inhibits MMP-9 secretion from human saphenous vein smooth muscle cells by inhibiting the RhoA/ROCK pathway and reducing MMP-9 mRNA levels. *FASEB J* 19: 804-806, 2005.



Copyright © 2023 Li *et al*. This work is licensed under a Creative Commons Attribution-NonCommercial-NoDerivatives 4.0 International (CC BY-NC-ND 4.0) License.